ACERP: Vol. 3, No. 4, (Fall 2017) 6-12

Advanced Ceramics Progress

Research Article

Journal Homepage: www.acerp.ir

Effect of the Sulfur Concentration on the Optical Band Gap Energy and Urbach Tail of Spray-Deposited ZnS Films

S. Ebrahimi, B. Yarmand*, N. Naderi

Department of Nanotechnology and Advanced Materials, Materials and Energy Research Center, Karaj, Iran.

P A P E R I N F O

Paper history:
Received 04 November 2017
Accepted in revised form 07 January 2018

Keywords:
ZnS
Spray pyrolysis
Zinc to Sulfur Molar Ratio
Band Gap Energy
Width of Urbach Tail

A B S T R A C T

Zinc Sulfide (ZnS) films were deposited through a simple and low cost spray pyrolytic technique by using mixed aqueous solutions of zinc nitrate and thiourea. The structural and optical properties of films were investigated as a function of initial (Zn:S) molar ratio in the precursor solution which varied between (1:1) and (1:3). X-ray diffraction (XRD) analysis revealed that wurtzite Zinc Oxide (ZnO) and cubic ZnS phases formed in the prepared film by the equal molar ratio of zinc to sulfur ions and only single cubic ZnS phase was appeared by increasing sulfur content in the precursor solution,. The transmittance spectra was measured by UV-Vis spectrophotometer indicated that by increasing the sulfur content, the transmittance of the films increased in the visible and near-infrared regions about 50% and the absorption edges shifted to the shorter wavelengths. As a result, the band gap energy (E_g) increased from 3.43 to 3.72 eV and the band tail width (E_u) decreased from 553 to 259 meV due to the phase composition and the decrement of structural defects. By extracting a linear relevance between the band gap energy and width of the band tail of ZnS, the optical band gap was estimated to be 3.977 eV at E_u= 0.

1. INTRODUCTION

Many research efforts have been pointed to the film deposition techniques and different types of materials that can often induce dramatic changes in the optical and electrical properties for using in various modern technologies of solid-state devices [1-3]. As a prominent functional II–VI compound semiconductor with a wide band gap (≈ 3.7 eV) [4], zinc sulfide (ZnS) has witnessed an explosion of interest over the last decade because of advances in controlled synthesis and unrivaled optical properties [5]. Under ambient conditions, ZnS crystallizes in two forms; zinc blend (cubic phase) and wurtzite (hexagonal phase) which have wide and direct band gaps about 3.54–3.6 and 3.74–3.87 (eV), respectively. Thus the wurtzite ZnS has large potential applications in electronics and optoelectronics. The cubic phase is stable at room temperature whereas the hexagonal phase is stable above 1020 °C at atmospheric pressure and metastable as a macroscopic phase. as Also, ZnS possesses significantly large exciton binding energy (approximately 40 MeV) compared to the low thermal energy (25 MeV at 273 K) that can be utilized for designing efficient room temperature exciton devices [6-9]. ZnS, in both bulk and film forms, is receiving ever increasing attention due to its broad spectrum of diverse application such as in photovoltaic technology [10], electroluminescence devices [11] and photo-catalysts [12] for a long time. In the optics area, ZnS can be used as an environmentally benign buffer layer for thin film solar cells, antireflective coating material in photovoltaic devices [13] and a dielectric filter due to its high transmittance in the visible range. In optoelectronics, it can be used as a light emitting diode in the blue to ultraviolet spectral region due to its direct wide band gap at room temperature [14, 15]. During the past decades, production of controlled and cost-effective materials is the key to employ them in practical applications. There are several advanced techniques for preparing ZnS films with unprecedented properties, such as chemical bath deposition (CBD) [16], thermal evaporation [17], radio frequency reactive sputtering [18], atomic layer deposition (ALD) [19], molecular beam epitaxy (MBE) [20], pulsed laser deposition (PLD) [21] and metal organic chemical vapor deposition (MOCVD) [22]. However, most of these techniques require vacuum conditions, precision instruments and also are not affordable. The technique

*Corresponding Author's Email: byarmand@merc.ac.ir (B. Yarmand)

of chemical spray pyrolysis is considered as a cheap technique to produce large area films. Many studies have been done over about three decades on spray pyrolysis processing and preparation of films since the pioneering work by Chamberlin and Skarman on cadmium sulfide (CdS) films for solar cells [23]. Therefore, due to the simplicity, ambient operating environment, relatively low cost and good productivity of this technique on a large scale, it offered a most attractive way for the formation of films of noble metals, metal oxides, spinel oxides, chalcogenides and superconducting compounds [13, 24]. As well as it has been successfully applied in preparing functional materials such as ZnO [25], MgO [26], SnO_2 [21] and $MnIn_xS_4$ [27] etc. Up to now, ZnS films deposited by spray pyrolysis have been investigated via several groups [28-32]. Primary studies on ZnS films by spray pyrolytic technique were performed by using $ZnCl_2$ and thiocarbamide (Tu) at fixed (Zn:S) molar ratio of (1:1) [2, 23, 33, 34]. Later, studies on the spray-deposited ZnS films prepared at different molar ratios of (Zn:S) in spray solution were appeared. They were introduced [29-32] that films grown from solution with same molar ratio of (Zn:S)= (1:1) had a cubic structure and band gap (Eg) values were 3.3–3.5 (eV). López et al. had considered that the zinc to sulfur molar ratio in the films grown at 500 °C increased from 0.8 to 0.92 varying the (Zn:S) in solution from (1:1) to (1:6) [30]. According to the Poornima et al. the ZnS films prepared at 450 °C were not well crystallized and ZnO phase was detected in the films grown from (1:0.5) and (1:1) solutions [32]. The researches on the ZnS films properties and formation, dependent on the molar ratio of precursors in solution at different deposition temperatures, remains still an important issue. So in this present research we have done a systematic study on the effect of the precursor's molar ratio on the structural and optical properties of sprayed ZnS layers deposited at a fixed temperature, 400 °C, without any capping agent for producing the films. It is expected that increasing sulfur content in the precursor solution causes a remarkable change on phase composition, structural defects, band gap energy and Urbach tails of ZnS films. To our best knowledge this is the first report considering Urbach tails in absorption spectra of ZnS films under affected of sulfur concentration.

2. MATERIALS AND METHODS

2.1. Materials and specimens preparation

Analytically pure zinc nitrate ($Zn(NO_3)_2.4H_2O$) and thiourea ($SC(NH_2)_2$) were used directly as received from Merck. All the chemicals were of analytical reagents grade and used as received without further purification. Deionized water was used throughout the process as a reaction medium in all the synthesis steps for dilution and sample preparation. The substrates used in this work were commercial soda-lime glass slides that were cleaned ultrasonically in ethanol for 10 min then washed with deionized water and finally dried.

2.2. Preparation of ZnS films

A home-made spray pyrolysis set-up had been used to prepare ZnS films. With spray pyrolysis, the solution was sprayed directly onto the clean substrates. A stream of gas (compressed air) was used for atomization of the solution through the nozzle. To preparing the precursor solutions, zinc nitrate and thiourea in three different molar ratio (Zn:S) of (1:1), (1:2) and (1:3) were dissolved in deionized water. Such solutions were used for the spray pyrolysis onto the pre-heated glass substrate maintained at 400 °C. The gas pressure and aqueous solution flow rate were kept constant at 3.5 bars and 4 $ml.min^{-1}$, respectively. Also, the nozzle to substrate distance was 25 cm. During spray pyrolysis process, when precursor solution droplets arrived close to the preheated substrates, the droplets decomposed thermally, which resulted into the forming a highly adherent ZnS film. No post-deposition annealing was given to these films and all the characteristics were studied in as-deposited samples. The different pyrolytic process parameters in film deposition are listed in Table 1. The schematic of the spray pyrolysis set-up applied in this study is presented in Fig. 1.

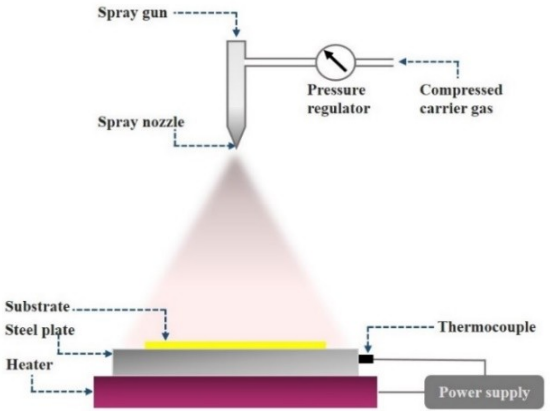

Figure 1. The schematic of the spray pyrolysis set-up

TABLE 1. Process parameters for the spray deposition of the films

Spray parameters	Optimum value
Substrate	Glass
Nozzle–substrate distance	25 (cm)
Zinc nitrate solution concentration	0.5 M
Solvent	Deionized water
Solution flow rate	4 $ml.min^{-1}$
Carrier gas	Compressed air
Substrate temperature	400 °C

2.3. Characterization of films

The crystalline structure of the films was confirmed by using high-resolution X-ray diffraction (XRD) with Cu Kα radiation (Kα= 1.54056 Å) (X'Pert PRO MPD, PANalytical, Netherlands) and the scanning angle 2θ was varied ranging 10° to 90°. Surfaces and cross-section morphologies of the films were observed by a field emission scanning electron microscope (FE-SEM, MIRA3, TESCAN, Czech). The chemical compositions of sprayed films were examined on the surface of the deposited films by using an energy dispersive spectrometer (EDS, OXFORD) equipped to the SEM. Optical absorbance spectrum was recorded by using UV–Vis spectrophotometer (Lambda25, Perkin Elmer, US) in the wavelength range of 300-1100 nm. All the measurements were performed at the room temperature.

3. RESULT AND DISCUSSION

3.1. Micro-structural and compositional properties

The effects of the molar ratio of sulfur to zinc ions on the crystallinity of the obtained films were studied by XRD. Fig. 2 shows XRD patterns of ZnS films prepared with diverse molar ratios of sulfur to zinc. The same amounts of the solution were used to deposit films with thicknesses of about 600 nm. The films grown from solutions with the molar ratio of (Zn:S)= (1:1) and (1:2) demonstrate poor crystallinity and contain zinc oxide (ZnO) as a secondary phase. The observed diffraction peaks at 31.9°, 34.5° and 36.4° match well with the wurtzite phase of ZnO crystal (JCPDS card No. 01-079-0205) for their intensity and peak position. For all the patterns, the results exhibit broad diffraction peak at the 2θ position of 29.5° related to the (111) refraction of the ZnS cubic phase. The peak has been indexed with the JCPDS card No. 01-079-0043. As obvious, increasing the amount of sulfur in ZnS lattice during deposition caused to increase the intensity of (111) peak and the observed peaks related to the ZnO phase slightly disappear. So, films produced from solution with the molar ratio of (Zn:S)= (1:3) introduced the single cubic phase of ZnS. As well as increasing the sulfur content in the structure draws on improving the crystallinity of the films. It is considered that diffraction peaks are significantly broadened essentially due to extremely small crystallite size. The mentioned findings prove that sufficient sulfur concentration is necessary for forming single phase of ZnS in spray pyrolysis process from aqueous solutions of zinc nitrate and thiourea complexes without using any capping agent. The observed results are in accordance with the data published earlier [29, 35-37].

SEM micrographs are indicated in Fig. 3 (a-b) for investigating the morphology and elemental composition of deposited ZnS film at 400 °C using Sulfur-rich solution.

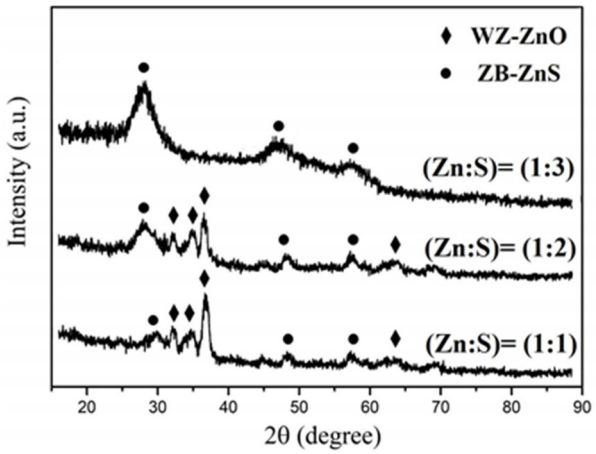

Figure 2. X-Ray diffraction patterns of ZnS films deposited at 400 °C with various molar ratios of (Zn: S)= (1:1), (1:2) and (1:3).

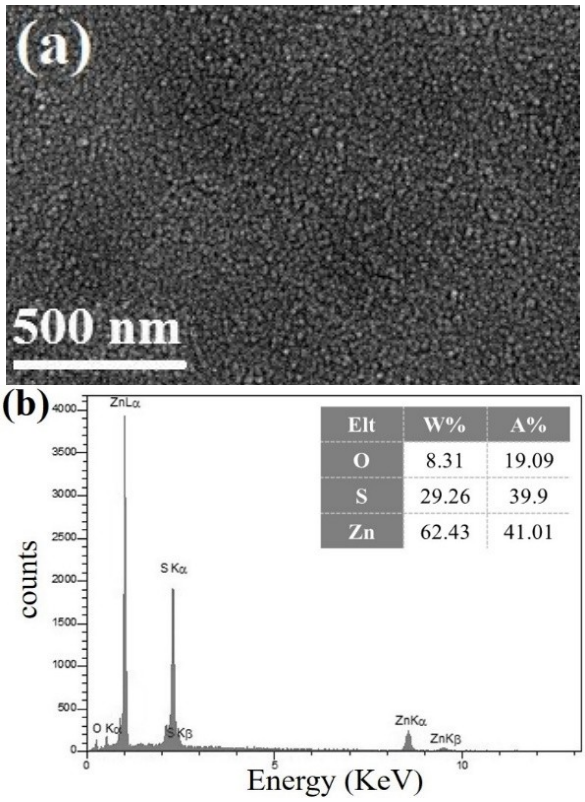

Figure 3. (a) SEM image and (b) Typical EDS spectra of deposited ZnS film at 400 °C with a molar ratio of (Zn: S)= (1:3)

Fig. 3a reveals uniform surface and dense structure. As well as ZnS film consists of smaller grains with the size about 4-5 nm. According to EDS analysis in Fig. 3b, the film contains low amount of oxygen due to the conditions of spray pyrolysis process. The flat area of film contains Zn and S that were found in a near-stoichiometric ratio with little sulfur deficiency. So S^{2-}/Zn^{2+} atomic ratio is 0.97 in the film deposited at 400

°C. It could be concluded that ZnS film from (1:3) solution has only cubic ZnS phase as shown in Fig. 2. EDS results are in accordance with that recorded by XRD as the film from S-rich solution contain crystalline cubic phase of ZnS.

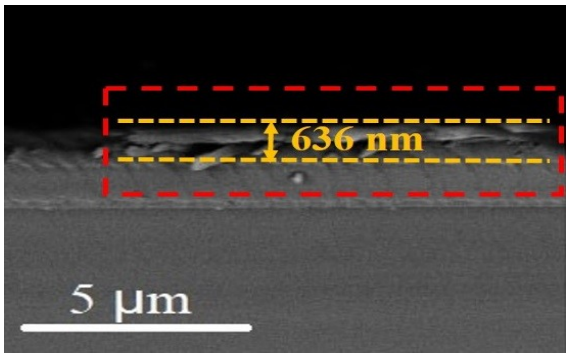

Figure 4. FE-SEM cross-sectional image of ZnS film deposited at 400 °C with molar ratio of (Zn: S)= (1:3)

Thickness of the ZnS film is determined by FE-SEM cross-sectional analysis. As illustrated in Fig. 4, the thickness of obtained film is about 636 nm.The films are produced in same amount of solution with the same deposition time and spray rate to obtaining nearly fixed thickness for all films.

3.2. Optical studies

The optical properties of ZnS films prepared by spray pyrolysis technique depend on the chemical composition of the precursor. Usually, an improved stoichiometry of precursor results in preparing of films with better optical transmission.

Fig. 5 shows the transmittance spectra against wavelength ranging from 300 to 1100 nm of sprayed ZnS films with different molar ratio of zinc to sulfur ions. It can be observed that transmittance of the films prepared from both solutions contained (1:1) and (1:2) of zinc to sulfur ions molar ratio have lower values varied from 15% to 35% in the visible and near-infrared regions. It is appeared due to the composed mixture of the ZnS and ZnO phases in their structure that proved by XRD results. Whereas obtained films from sulfur-rich solution (1:3) possess high specular transmittance around 65% in the visible and near-infrared spectral region, these observations are in good agreement with results found by other researchers [2, 38, 39]. Also from Fig. 5, it can be concluded that all the films have high absorption around the ultra-violent regime (320-360 nm).

Fig. 6 illustrates the relation between the absorption coefficient (α) and the photon energy (hυ), where h is Planck's constant and υ is the frequency of the radiation.

$$\alpha = -Ln\ (T)/t \qquad (1)$$

The thickness of the film (t) has been determined by FE-SEM cross-sectional images. The direct relationship between the absorption coefficient and sulfur concentration for wavelength values smaller than the cutoff wavelength is proved by these absorption spectra.

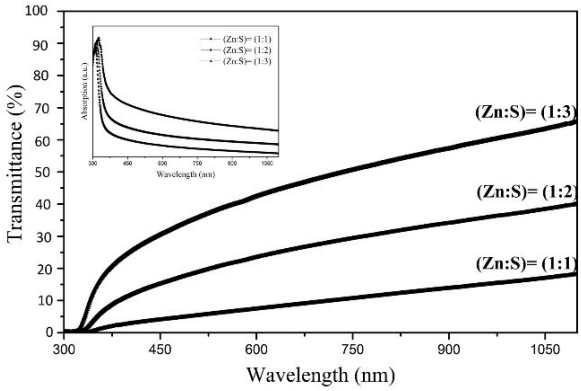

Figure 5. Transmittance spectra vs. wavelength of ZnS films deposited at 400 °C with various molar ratios of (Zn: S)= (1:1), (1:2) and (1:3)

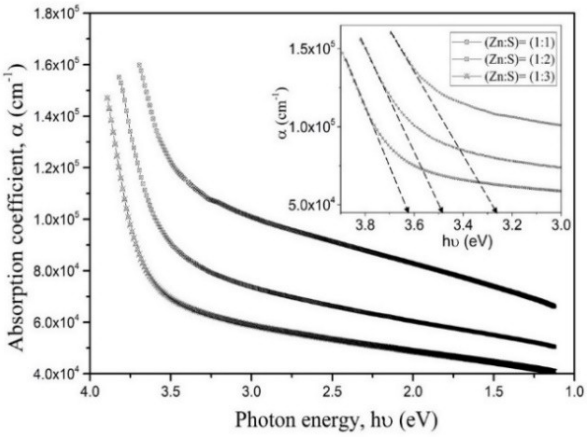

Figure 6. The relation between the absorption coefficient (α) and the photon energy (hυ) of ZnS deposited films at 400 °C with various molar ratios of (Zn: S)= (1:1), (1:2) and (1:3)

For calculating the value of optical band gap energy, the relationship between the absorption coefficient (α) and the energy of the incident light (hυ) is given by Tauc equation:

$$(\alpha h\upsilon)^{1/n} = \alpha_0(h\upsilon - E_g) \qquad (2)$$

Where, E_g is the optical band gap energy, α_0 is the edge width parameter and n is equal to 2 for the direct band gap semiconductors, such as ZnS. The direct optical band gap values of the ZnS films have been estimated by plotting a graph between $(\alpha h\upsilon)^2$ versus hυ shown in Fig. 7. The band gap energy has been evaluated by extrapolating the straight line portion of the graph to the hυ axis (maximum transmission, i.e. α= 0). The

estimated values of the optical band gap energy of the films are listed in Table 2. Apparently, the calculated band gap values for preparing films from both (Zn:S) molar ratios of (1:1) and (1:2) have minimum values. Also, obtained band gap energies for both solutions are lower than the bulk crystal (E_g= 3.65 eV); which can be ascribed to the sulfur deficiency [40]. This result can be associated with the presence of zinc oxide (as proved by XRD profiles) in which an energy gap is very close to the ZnS (E_g= 3.24 eV) [41]. The general trend of the band gaps for ZnS deposited films from solutions with different molar ratio increase as sulfur content of the solution increased.

As realized from Fig. 7, the band gap energy of the obtained film from solution with the excess amount of the sulfur is approximately equal to the band gap energy of the ZnS cubic phase which obtained in XRD analysis. The increment in the transmittance and band gap energy with increasing sulfur concentration is possible due to the changing of phase morphology, the improving of crystallinity and stoichiometry of the films. It is important to mention that the effect of thickness on the transmittance of the films is less important than the effect of chemical composition (as summarized in Table 2).

TABLE 2. The values of the optical band gap energy (E_g) and the band tail width (E_u) of ZnS deposited films at 400 °C with various molar ratios of (Zn: S)= (1:1), (1:2) and (1:3)

molar ratio of (Zn:S)	Thickness (nm)	Wavelength of absorption edge (nm)	E_g (eV)	E_u (meV)
(1:1)	615	360	3.43	553
(1:2)	628	343	3.59	396
(1:3)	636	332	3.72	259

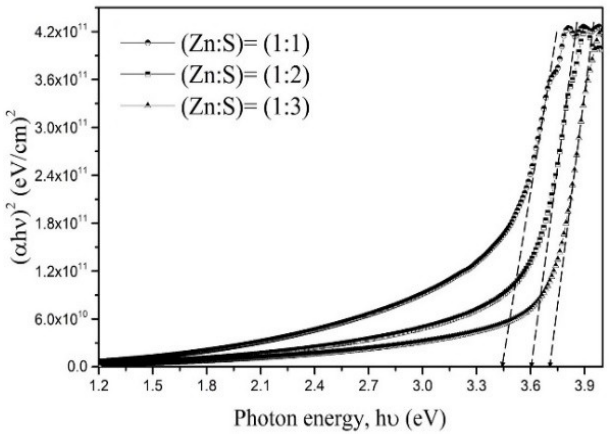

Figure 7. The variation of $(\alpha h\upsilon)^2$ as a function of photon energy (hυ) for determining of the optical band gap energy for ZnS deposited films at 400 °C with various molar ratios of (Zn: S)= (1:1), (1:2) and (1:3)

In the semiconductors and insulators, the spectral dependence of the absorption edge on the low photon energy range follows the empirical Urbach rule given by:

$$\alpha = \alpha_0 \exp\left(\frac{h\upsilon}{Eu}\right) \quad (3)$$

Where α_0 is a constant, E_u is often interpreted as the width of the tail of localized states in the band gap. The exact cause of the Urbach exponential tails has phonons, impurities, excitons and structural disorders in the materials [42-44]. In the near absorption edge, the variation of $\ln \alpha$ against the photon energy is induced in Fig. 8 for ZnS obtained films in various molar ratios of zinc to sulfur. The width of Urbach tail (E_u) for all the films was computed from the reciprocal gradient of the straight line and presented in Table 2. It is considered that increasing of sulfur content in ZnS lattice draws on decreasing E_u values. The behavior of E_u can be attributed to the decreasing disordered atoms and defects in the structural bonding and improving the structural crystallinity along that increasing amount of sulfur in deposited films. The disorder and defects can introduce localized states at or near the conduction band level leading to increasing the Urbach energy [45].

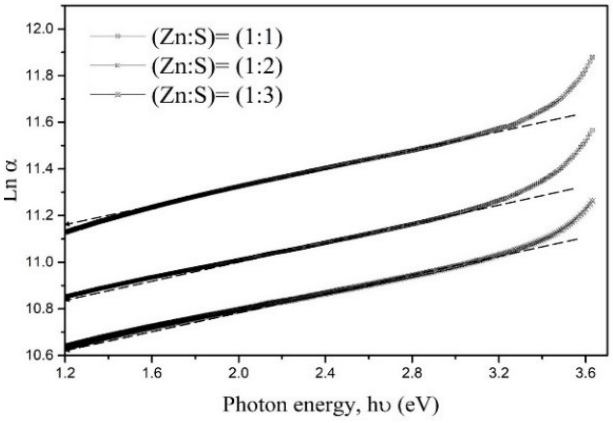

Figure 8. The variation of $\ln \alpha$ against the photon energy (hυ) of ZnS deposited films at 400 °C with various molar ratios of (Zn: S)= (1:1), (1:2) and (1:3).

Furthermore, to study of the Urbach tail of the films, the relationship between the band gap energy and the width of Urbach tail was investigated for the first time in the case of ZnS films with diverse molar ratio of the zinc to sulfur. According to the Fig. 8, it can be confirmed that the Urbach tail decreases as the optical band gap increases. Also, there is a linear correlation between band gap and Urbach tail, therefor a linear fit was extracted. The experimental equation from this linear fitting is presented as:

$$E_g = 3.977 - 0.987\, E_u \quad (4)$$

The average value of the constant parameter (α_0) of equation 3 can be evaluated from the linear fitting of Fig. 9. As well as the equation introduce the band gap energy in the absence of band tailing which in the case of the ZnS films, optical band gap (E_g) is equal to 3.977 (eV) at E_u= 0. Such a linear relation between band gap energy and the Urbach tail was found for other semiconductors [43, 46, 47].

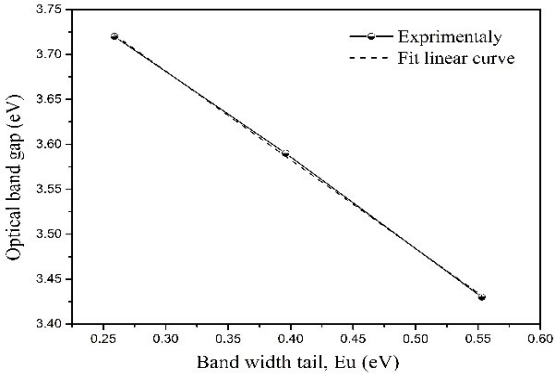

Figure 9. The relationship between the band gap energy (E_g) and the width of Urbach tail (E_U) of ZnS deposited films at 400 °C with various molar ratios of (Zn: S)= (1:1), (1:2) and (1:3)

4. CONCLUSION

In summary, a low-cost, continuous, easy-controllable spray pyrolysis method has been used to deposit ZnS films. A systematic study on the impact of main spray pyrolysis technological parameter such as molar ratio (Zn:S) of precursor, (1:1), (1:2) and (1:3), at the fixed substrate temperature about 400 °C, on structural and optical properties of ZnS films was presented. Relatively good crystallinity and ZnS cubic single phase in sulfur-rich solution was obtained at spray rate of 4 $ml.min^{-1}$. The band gap energy was computed through the absorption coefficient and found that by increasing sulfur concentration up to three times of zinc content in the ZnS lattice, the transmittance and values of the band gap energy slightly increased due to improving of crystallinity and producing the single ZnS cubic phase. From the plot of the natural logarithm of the absorption coefficient against the incident photon energy, it was observed that this tailing confirms Urbach rule. The width of the tail decreased by increasing sulfur content because of the reduction of impurities and disorders. Finally, a linear dependence between the band gap energy and the width of Urbach tail was appreciated for the first time in the case of ZnS deposited films in different molar ratios of zinc to sulfur.

5. ACKNOWLEDGMENTS

This research has been supported with research grant (NO.: 247383) by Materials and Energy Research Center (MERC), Karaj, Iran.

REFERENCES

1. Goudarzi, A., Motedayen Aval, G., Park, S.S., Choi, M.C., Sahraei, R., Ullah, M.H., Avane, A. and Ha, C.S., "Low-temperature growth of nanocrystalline Mn-doped ZnS thin films prepared by chemical bath deposition and optical properties", ***Chemistry of Materials,*** Vol.21, (2009), 2375-2385.
2. Elidrissi, B., Addou, M., Regragui, M., Bougrine, A., Kachouane, A. and Bernède, J.C., "Structure, composition and optical properties of ZnS thin films prepared by spray pyrolysis", ***Materials Chemistry and Physics,*** Vol. 68, (2001), 175-179.
3. Saeed, N.M., "Structural and optical properties of ZnS thin films prepared by spray pyrolysis technique", ***Journal of Al-Nahrain University,*** Vol. 14, (2011), 86-92.
4. Yamaga, S., Yoshikawa, A. and Kasai, H., "Electrical and optical properties of donor doped ZnS films grown by low-pressure MOCVD", ***Journal of Crystal Growth,*** Vol. 86, (1988), 252-256.
5. Fang, X., Bando, Y., Meiyong Liao, M., Zhai, T., Gautam, U.K., Li, L., Koide, Y. and Golberg, D., "An efficient way to assemble ZnS nanobelts as ultraviolet-light sensors with enhanced photocurrent and stability", ***Advanced Functional Materials,*** Vol. 20, (2010), 500-508.
6. Salem, J.K., Hammad, T.M., Kuhn, S., Draaz, M.A., Hejazy, N.K. and Hempelmann, R., "Structural and optical properties of Co-doped ZnS nanoparticles synthesized by a capping agent", ***Journal of Materials Science: Materials in Electronics,*** Vol. 25, (2014), 2177-2182.
7. Wang, X., Huang, H., Liang, B., Liu, Z., Chen, D. and Shen, G., et al., "ZnS nanostructures: synthesis, properties, and applications", ***Critical Reviews in Solid State and Materials Sciences,*** Vol. 38, (2013), 57-90.
8. Zhai, T., Li, L., Ma, Y., Liao, M., Wang, X., Fang, X., Yao, J., Bando, Y. and Golberg, D., "One-dimensional inorganic nanostructures: synthesis, field-emission and photodetection", ***Chemical Society Reviews,*** Vol. 40, (2011), 2986-3004.
9. Dong, L., Liu, Y., Zhuo, Y. and Chu, Y., "General route to the fabrication of ZnS and M-Doped (M = Cd^{2+}, Mn^{2+}, Co^{2+}, Ni^{2+} and Eu^{3+}) ZnS nanoclews and a study of their properties", ***European Journal of Inorganic Chemistry,*** Vol. 2010, (2010), 2504-2513.
10. Bär, M., Ennaoui, A., Klaer, J., Kropp, T., Sáez-Araoz, R., Allsop, N., Lauermann, I., Scho, H.W. and Lux-Steiner, M.C., "Formation of a ZnS⁄Zn(S,O) bilayer buffer on $CuInS_2$ thin film solar cell absorbers by chemical bath deposition", ***Journal of Applied Physics,*** Vol. 99, (2006), 064911.
11. Sohn, S. and Hamakawa, Y., "Excitation and deexcitation of ac-driven thin-film ZnS electroluminescent devices", ***Journal of Applied Physics,*** Vol. 72, (1992), 2492-2504.
12. Bang, J.H., Helmich, R.J. and Suslick, K.S., "Nanostructured ZnS:Ni^{2+} photocatalysts prepared by ultrasonic spray pyrolysis", ***Advanced Materials,*** Vol. 20, (2008), 2599-2603.
13. Zeng, X., Pramana, S.S., Batabyal, S.K., Mhaisalkar, S.G., Chena, X. and Jinesh, K.B., "Low temperature synthesis of wurtzite zinc sulfide (ZnS) thin films by chemical spray pyrolysis", ***Physical Chemistry Chemical Physics,*** Vol. 15, (2013), 6763-6768.
14. Zhang, L., Qin, D., Yang, G. and Zhang, Q., "The investigation on synthesis and optical properties of ZnS: Co nanocrystals by using hydrothermal method", ***Chalcogenide Letters,*** Vol. 9, (2012) 93-98.
15. Cao, J., Yang, J., Zhang, Y., Wang, Y., Yang, L., Wang, D., Liu, Y., Liu, X. and Xie, Z., "XAFS analysis and luminescent properties of ZnS:Mn^{2+} nanoparticles and nanorods with cubic

and hexagonal structure", ***Optical Materials,*** Vol. 32, (2010), 643-647.

16. Sartale, S., Sankapal, B., Lux-Steiner, M.C. and Ennaoui, A., "Preparation of nanocrystalline ZnS by a new chemical bath deposition route", ***Thin Solid Films,*** Vol. 480, (2005), 168-172.
17. Durrani, S., Al-Shukri, A.M., Iob, A. and Khawaja, E.E., "Optical constants of zinc sulfide films determined from transmittance measurements", ***Thin Solid Films,*** Vol. 379, (2000), 199-202.
18. Shao, L. X., Chang, K. H.and Hwang, H. L., "Zinc sulfide thin films deposited by RF reactive sputtering for photovoltaic applications", ***Applied Surface Science,*** Vol. 212, (2003) 305-310.
19. Tanskanen, J.T., Bakke, J.R., Bent, S. and Pakkanen, T., "ALD growth characteristics of ZnS films deposited from organozinc and hydrogen sulfide precursors", ***Langmuir,*** Vol. 26, (2010), 11899-11906.
20. Yokoyama, M., Kashiro, K.I. and Ohta, S.I., "High quality zinc sulfide epitaxial layers grown on (100) silicon by molecular beam epitaxy", ***Applied Physics Letters,*** Vol. 49, (1986), 411-412.
21. Yano, S., Schroeder, R., Ullrich, B. and Sakai, H., "*Absorption and photocurrent properties of thin ZnS films formed by pulsed-laser deposition on quartz*", ***Thin Solid Films,*** Vol.423, (2003), 273-276.
22. Dean, P., Pitt, A.D., Skolnick, M.S., Wright, P.J. and Cockayne, B., "Optical properties of undoped organometallic grown ZnSe and ZnS", ***Journal of Crystal Growth,*** Vol. 59, (1982), 301-306.
23. Chamberlin, R. and Skarman, J., "Chemical spray deposition process for inorganic films", ***Journal of the Electrochemical Society,*** Vol. 113, (1966), 86-89.
24. Shinde, S.D., Patil, G.E., Kajale, D.D., Gaikwad, V.B. and Jain, G.H., "Synthesis of ZnO nanorods by spray pyrolysis for H_2S gas sensor", ***Journal of Alloys and Compounds,*** Vol. 528, (2012), 109-114.
25. Addou, M., Moumin, A., B, E., Regragui, M., Bougrine, A., Kachouane, A. and Monty, C., "Structural, optical and electrical properties of undoped and indium doped zinc oxide prepared by spray pyrolysis", J***ournal de Chimie Physique et de Physico-Chimie Biologique,*** Vol. 96, (1999), 232-244.
26. Boo, J. H., Lee, S.B., Yu, K.S., Koh, W. and Kim, Y., "Growth of magnesium oxide thin films using single molecular precursors by metal–organic chemical vapor deposition", ***Thin Solid Films,*** Vol. **341, (**1999), 63-67.
27. Sharma, R., Lakshmikumar, S.T., Singh, G. and Rastogi, A.C., "Photoluminescence in manganese indium sulphide thin films deposited by chemical spray pyrolysis", ***Materials Chemistry and Physics,*** Vol. 92, (2005), 240-244.
28. Ben Nasrallah, T., Amlouk, M., Bernède, J.C. and Belgacem, S., "Structure and morphology of sprayed ZnS thin films", ***Physica Status Solidi (A),*** Vol. 201, (2004), 3070-3076.
29. Dedova, T., Krunks, M., Volobujeva, O. and Oja, I., "ZnS thin films deposited by spray pyrolysis technique", ***Physica Status Solidi (C),*** Vol. 2, (2005), 1161-1166.
30. Lopez, M.C, Espinos, J.P., Martín, F., Leinen, D. and Ramos-Barrado, J.R., "Growth of ZnS thin films obtained by chemical spray pyrolysis: The influence of precursors", ***Journal of Crystal Growth,*** Vol. 285, (2005), 66-75.
31. Hernandez-Fenollosa, M.A, López, M.C., Donderis, V., González, M., Marí., B. and Ramos-Barrado, J.R., "Role of precursors on morphology and optical properties of ZnS thin films prepared by chemical spray pyrolysis", ***Thin Solid Films,*** Vol. 516, (2008), 1622-1625.
32. Poornima, N., Jose, A., Kartha, C.S. and Vijayakumar, K.P., "Composition and conductivity-type analysis of spray pyrolysed ZnS thin films using photoluminescence", ***Energy Procedia,*** Vol. 15, (2012), 347-353.
33. Afifi, H., Mahmoud, S. and Ashour, A., "Structural study of ZnS thin films prepared by spray pyrolysis", ***Thin Solid Films,*** Vol. 263, (1995), 248-251.
34. Su, B. and Choy, K., "Electrostatic assisted aerosol jet deposition of CdS, CdSe and ZnS thin films", ***Thin Solid Films,*** Vol. 361, (2000), 102-106.
35. Tohge, N., Tamaki, S. and Okuyama, K., "Formation of fine particles of zinc sulfide from thiourea complexes by spray pyrolysis", ***Japanese Journal of Applied Physics,*** Vol. 34, (1995), L207.
36. Sharma, H.K., Shukla, P. and Agrawal, S., "Effect of sulphur concentration on the structural and electronic properties of ZnS nanoparticles synthesized using chemical precipitation method", ***Journal of Materials Science: Materials in Electronics,*** Vol. 28, (2017), 6226-6232.
37. Dedova, T., Krunks, M., Gromyko, I., Mikli, V., Sildos, I., Utt, K. and Unt, T., "Effect of Zn:S molar ratio in solution on the properties of ZnS thin films and the formation of ZnS nanorods by spray pyrolysis", ***Physica Status Solidi (A),*** Vol. 211, (2014), 514-521.
38. Lindroos, S., Kanniainen, T. and Leskelä, M., "Growth of zinc sulfide thin films by the successive ionic layer adsorption and reaction (SILAR) method on polyester substrates", ***Materials Research Bulletin,*** Vol. 32, (1997), 1631-1636.
39. Johnston, D., Carletto, M.H., Reddy, K.R.T., Forbes, I. and Miles, R.W., "Chemical bath deposition of zinc sulfide based buffer layers using low toxicity materials", ***Thin Solid Films,*** Vol. 403, (2002), 102-106.
40. Barreca, D., A. Gasparotto, A., Tondello, E., Sada, C., Polizzi, S. and Benedetti, A., "Nucleation and growth of nanophasic CeO_2 thin films by Plasma-Enhanced CVD", ***Chemical Vapor Deposition,*** Vol. 9, (2003), 199-206.
41. Ayouchi, R., Martin, F., Leinen, D., Ramos-Barrado, J.R., "Growth of pure ZnO thin films prepared by chemical spray pyrolysis on silicon", ***Journal of Crystal Growth,*** Vol. 247, (2003), 497-504.
42. Urbach, F., "The long-wavelength edge of photographic sensitivity and of the electronic absorption of solids", ***Physical Review,*** Vol. 92, (1953), 1324.
43. Ikhmayies, S.J. and Ahmad-Bitar, R.N., "A study of the optical bandgap energy and Urbach tail of spray-deposited CdS: In thin films", ***Journal of Materials Research and Technology,*** Vol. 2, (2013), 221-227.
44. Rothwarf, A., Meakin, J. and Bamett, A., "Polycrystalline and amorphous thin films and devices", 1980, Academic Press, New York.
45. Yakuphanoglu, F., Ilican, S., Caglar, M. and Çağlar, Y.Y., "The determination of the optical band and optical constants of non-crystalline and crystalline ZnO thin films deposited by spray pyrolysis", ***Journal of Optoelectronics and Advanced Materials,*** Vol. 9, (2007), 2180-2185.
46. Aly, K., et al., "Optical properties of Ge–As–Te thin films", ***Physica B: Condensed Matter,*** Vol. 406, (2011), 4227-4232.
47. Melsheimer, J. and Ziegler, D., Band gap energy and Urbach tail studies of amorphous, partially crystalline and polycrystalline tin dioxide, ***Thin Solid Films,*** Vol. 129, (1985), 35-47.